

A mechanism for early branching in lung morphogenesis

Sharon R. Lubkin, J. D. Murray

Department of Applied Mathematics, Box 352420, University of Washington, Seattle, WA 98195-2420, USA
e-mail: lubkin@amath.washington.edu

Received 13 October 1994; received in revised form 21 February 1995

Abstract. The lung is a highly branched fluid-filled structure, that develops by repeated dichotomous branching of a single bud off the foregut, of epithelium invaginating into mesenchyme. Incorporating the known stress response of developing lung tissues, we model the developing embryonic lung in fluid mechanical terms. We suggest that the repeated branching of the early embryonic lung can be understood as the natural physical consequence of the interactions of two or more plastic substances with surface tension between them. The model makes qualitative and quantitative predictions, as well as suggesting an explanation for such observed phenomena as the asymmetric second branching of the embryonic bronchi.

Key words: Lung – Pattern formation – Morphogenesis – Fetal development

1 Introduction: biology of the embryonic lung

The development of the lung is immensely complex but can be divided into four phases. In the *embryonic* stage, which spans the first few weeks of gestation in the human, the basic bronchial tree is laid out, and the lung lobes are defined. An initial lung primordium buds off the foregut after week 3, and in the next week, divides at its tip into the two lung buds which will become the right and left lungs. The two lung buds elongate and branch again, the left bud into two more branches, and the right into three (Fig. 1). These tips continue to grow and split, until, by the end of the embryonic period, the basic lobar structure and the bronchi are established. The *glandular* or *pseudoglandular* stage begins after 5–7 weeks, and lasts until weeks 14–16. It is characterized by the formation of the bronchioles, by continued branching of the bronchial tree, until there are between 16 and 25 generations of branching. The *canalicular* stage follows, until week 24–26, at which time the *saccular*

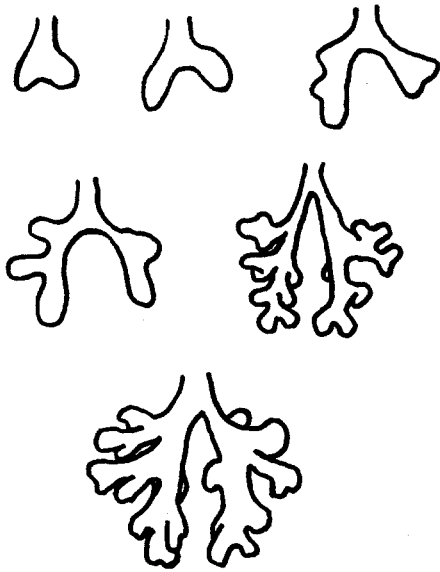


Fig. 1. Early embryonic lung epithelium-mesenchyme boundary at different times, developmental weeks 4–6. Adapted from (Hodson 1977; Nelson 1985)

phase begins, and the acini have begun to form (Crystal 1991; Nelson 1985). It is primarily the embryonic stage of development with which we shall be concerned in this study, since it consists of the development and interaction of a minimal number of different types of tissues, and therefore is the most tractable to model.

The embryonic lung can be thought of as an inside-out organ, a clump of mesenchyme which is invaded by invaginating epithelium. As such, it is developmentally and structurally quite similar to the salivary gland, kidney, and other branched organs. The hollow finger of epithelium is filled with fluid, primarily secreted by the epithelium, but continuous with the amniotic fluid, and undergoes repeated tip-splitting until it becomes the highly branched structure which we think of as the bronchial tree. The mature lung has a scale-invariance to its branching from 0.1 mm to 10 mm, which optimizes the fluid flow from the trachea down to the smallest bronchioles (Weibel 1991). However, this optimization of branching sizes occurs in the later stages of development, possibly in response to the mechanical stresses caused by the fetal breathing movements, which have not been observed before week 10 (Crystal et al. 1991), and which are essential to the proper development of the lung.

The branch structure of the lung is highly consistent at the level of the largest bronchi, to the extent that each lobe, defined by a bronchus, has a name. However, developmental variations are common (Hodson 1977), and the later the generation of branching (the smaller the branch), the more

variation is seen. (This is to be expected, even at the statistical level: there are, at each generation g , 2^g branches of the airways, so we expect to observe more variations at large g .)

The form of the lung is described consistently as arising out of repeated dichotomous branching: the airways contain essentially no junctions where a single passage splits into three daughter passages, and it is believed (Alescio and Cassini 1962) that the lung never develops by side-branching except in the highly artificial case of transplantation, that is grafting of side-branches. The absence of trifurcating branches and side-branching are examples of developmental constraints predicted by the “morphogenetic rules” postulated by Oster et al. (1988). (For an extended discussion, see Murray 1989.) Thus an appropriate model mechanism should form pattern almost exclusively by dichotomous tip-splitting.

The embryonic lung, like other branched organs such as the salivary gland, is developmentally self-sufficient, that is, it can branch and differentiate normally *in vitro*. The branching and growth are controlled by chemical and mechanical interactions between the epithelium and mesenchyme. The chemical aspects of branching development have been extensively studied (for reviews, see Jetten 1991; McGowan 1992), but the mechanical aspects are very much less widely studied, and shed more light on the actual *form* of the branched organ than is possible with the extensive (and important) chemical mechanisms. Studies of ligation and tracheostomy *in vivo* (Alcorn et al. 1977; Fewell et al. 1983; Moessinger et al. 1990) dramatically and quantitatively demonstrate the effect of variable luminal pressure on developing lung morphology. In the later stages of development, it is clear that high luminal pressure strongly stimulates growth, while low pressure leads to abnormally small lungs.

In vitro experiments have dramatically demonstrated the responsiveness of fetal lung fibroblasts (Bishop et al. 1993) and mixed lung tissues (Liu et al. 1992) to cyclic mechanical deformation mimicking fetal breathing movements. For example, cyclic deformation of 10% strain for 2 days increased fibroblast number by 39% over control (Bishop et al. 1993). The greater the average stress/strain level, the greater was the increase in growth rate. This strong responsiveness points to an important role of the fetal breathing movements in mechanically stimulating lung development; it also highlights the important role of general mechanical aspects of development of the lung.

Epithelium is also strongly stress-responsive. It is typical of epithelium to maintain a uniform thickness, despite substantial deformations and stresses. It is also characterized by its tendency to adapt to the mechanical stresses imposed on it by deforming and undergoing mitosis, so as to maintain a uniform residual tangential stress (Takeuchi 1979; Kolega 1981).

It is this strong response of embryonic tissues' growth rate to mechanical stress, and the tendency of epithelium to maintain a fairly uniform residual tangential stress, that suggests a mechanical description of the tissue growth and deformation of branching development.

2 Mechanical model of tissue deformations

The simplest mathematical interpretation of the stress-growth response of the *in vitro* studies is that there is an approximately linear relationship between the average stress on lung mesenchyme and its growth rate. Geometrically, growth rate is equivalent to strain rate, and therefore our model will assume a linear relation between stress and strain rate of the lung mesenchyme. This is exactly equivalent to the stress-strain rate description of fluid flow; the proportionality factor, μ , is called the tissue's viscosity. Note that on the fast time scale of breathing movements, lung tissues behave viscoelastically and not as a fluid. However, on the slow time scale of growth and development – days, rather than seconds – the mesenchyme behaves as a viscous fluid, averaging the fast-time-scale stresses. (The luminal/amniotic fluid which fills the lung behaves as a viscous fluid on any time scale.)

The tendency of epithelium, on the time scale of development, to maintain a uniform tangential stress is mechanically equivalent to the behavior of a surface tension between two fluids.

We have thus arrived at a mechanical description of the deformation and growth of lung tissues during development. The mechanisms by which the tissues sense stresses and respond with deformation of their cytoskeletons,

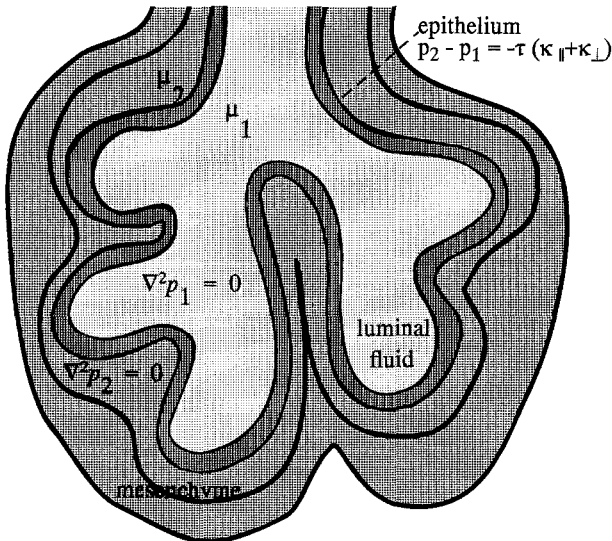


Fig. 2. The lung is modeled as a collection of fluids with interfaces between them. The amniotic fluid, naturally considered a fluid, is the innermost, and the mesenchyme, which could be considered either as a single fluid component or as two different fluids with different consistencies, is outside. Between the amniotic fluid and mesenchyme is epithelium, its thinness exaggerated in this drawing, which behaves like a surface tension τ between two fluids. The viscosity μ_1 of the luminal fluid is negligible (close to water) compared to that of the mesenchyme, μ_2

altered mitotic rates, and altered rates of synthesis and degradation of extracellular matrix (ECM) and basement membrane are another question entirely, but the facts of the known tissue responses to stress lead us to a useful and powerful mechanical description.

We consider the embryonic lung to consist of two fluids of very different viscosities, luminal/amniotic fluid and mesenchyme, separated by a “skin” of surface tension, the epithelium (Fig. 2). In Sect. 4 we will consider the implications of modeling the lung as three fluids. The viscosity of the luminal fluid is clearly negligible compared to that of the mesenchyme, since the former fluid is close to water, and deforms almost immediately, whereas mesenchyme has a viscosity many orders of magnitude greater (see Appendix).

3 Mathematical description of the model

The flow of developing tissues is slow, and is characterized by very low Reynolds number (see Appendix). Thus it can be described by Stokes’ equation,

$$\nabla p = \mu \nabla^2 u \quad (1)$$

for each fluid, where p is pressure, u is velocity (vector), and μ , viscosity (Landau and Lifshitz 1959). We assume a constant intrinsic growth rate c of the mesenchyme,

$$\nabla \cdot u = c \quad (2)$$

and incompressibility of the amniotic/luminal fluid,

$$\nabla \cdot u = 0 \quad (3)$$

Either of these assumptions reduce Stokes’ equation to Laplace’s equation for pressure in each fluid:

$$\nabla^2 p = 0 \quad (4)$$

Epithelium is considered to be thin, and is described by a geometric relation between the pressure jump δp across it, its surface tension τ , and its two curvatures κ_{\perp} and κ_{\parallel} ,

$$\delta p = -\tau(\kappa_{\perp} + \kappa_{\parallel}) \quad (5)$$

When one fluid is driven into a less viscous fluid, the interface between them remains relatively smooth. However when a fluid is driven into a *more* viscous fluid, an initially planar interface between them becomes unstable. This instability generates fingers of a characteristic range of wavelengths if the surface tension is nonzero. In certain arrangements, these fingers in turn become unstable by tip splitting, and often a branched structure can result.

The most common experimental and theoretical configuration for studying this viscous fingering is flow in a linear Hele-Shaw cell (Saffman and

Taylor 1958). The two-dimensional chamber has parallel plates maintained at a constant gap b and rigid side walls at a distance a from each other. In this simplified system, there is a single nondimensional control parameter,

$$B = \frac{\pi^2 b^2 \tau}{3 a^2 U \delta\mu} \quad (6)$$

where U is the average velocity of the interface and $\delta\mu$ the difference in viscosities across the interface (see Sect. 4.1). When B is large, that is, at low velocity, high surface tension, or low difference in viscosities, a planar interface is stable. When B is sufficiently smaller, an initially planar interface becomes unstable to various wavelengths, and fingers develop. In the Saffman-Taylor configuration, the only stable interface in this parameter range appears to be a single finger, of width generally close to $a/2$. If B decreases still further, one observes tip splitting, tip wander, and other phenomena, but in general, a single finger dominates. If a tip splits in two, one tip will be seen to grow at the expense of the other (Kessler et al. 1988).

Another configuration of a Hele-Shaw cell that has been studied, although less widely than the Saffman-Taylor finger, is radial flow. Experiments show that as the less viscous fluid is driven into the more viscous fluid from the center of the cell, an initially circular interface goes unstable with a characteristic wavelength that depends on the control parameter B , but also on the radius of the circular interface. At larger radii, the fingers in turn go unstable, and split. At very low values of B , the structure becomes highly branched (Kessler et al. 1988).

While the lung is clearly a three-dimensional organ, we believe that some of the major branching aspects can be seen in a simplified two-dimensional model. Numerical simulations of a three-dimensional version are considerably more complex and computationally intensive, and are currently under investigation. We shall therefore simplify the analysis of our fluid model, by reducing it to two dimensions by a Hele-Shaw approximation. This has the dual advantages of placing the model in the context of a well-studied physical phenomenon, and also of immediately leading to verifiable experimental predictions, since the technique of two-dimensional culture already exists.

The justifiable *ansatz* of a parabolic profile between the parallel plates, where b is small, leads to an asymptotic form of Stokes' equation, Darcy's law:

$$\nabla p = - \frac{12\mu}{b^2} u \quad (7)$$

where u and ∇p are now considered to be vectors in R^2 .

It remains to specify a driving force for the fluid motion, or a pressure driving the deformation of the tissues. Pressures in the lung have been measured in the latter stages of development in fetal sheep, and it is found that there is a positive pressure of 1.5–3 mm Hg over amniotic pressure in the trachea, and a negative pressure of 1–2 mm Hg in the pleura (Fewell and

Johnson 1983; Vilos and Liggins 1982). Thus there is a total pressure across the epithelium-mesenchyme interface of approximately 5 mm Hg, at least in the later stages of development (Alcorn et al. 1977). There is no experimental evidence of pressure across this interface in the embryonic lung, but based on the evidence at later stages, it is not an unreasonable assumption for this model.

However, this transpleural pressure is too small, by an order of magnitude, to account for the observed growth rate (see Appendix for discussion of parameter estimates). The largest portion of the driving force must be due to the general expansion of the embryo during this period and to an intrinsic growth rate of the lung tissues. Lung explants develop fairly normally *in vitro*, without any externally imposed force. Generally the lumen closes *in vitro*, allowing for a positive luminal pressure. The intrinsic growth rate of the mesenchyme acts as a driving force giving an overall expansion (Eq. 2). Furthermore, the thoracic cavity is grossly enlarging, and this overall expansion has the mathematical effect of a moving boundary, and the same mechanical effect as the motion of a piston drawing fluid. We expect that the natural driving force *in vivo* is a combination of the intrinsic growth rate, the transpleural pressure, and the general expansion of the thoracic cavity. In the initial analysis to follow, we shall omit the source term c of the growth of mesenchyme, and explore only the effect of the boundary conditions and driving pressure.

An expanding lung is not completely unrestrained, *in vivo*, since there are the other organs of the early embryo to consider, such as the heart and the esophagus, which will clearly be obstacles to deformation or flow of a fluid. Thus there will be some cavity into which the deforming lung may grow, but its exact shape is not at all clear, nor how rigid are its boundaries. Moreover, the shape of the space (or simply of the pleural cavity) changes over time, as development proceeds. Analysis of the model could tell us something about the boundary conditions on the growing embryonic lung.

4 Linear analysis of the pattern formation

4.1 Two fluids

Consider the case where there are two fluids in a Hele-Shaw cell, of different viscosities, with an interface Γ between them, possessing surface tension τ . Then the condition relating the curvature and the surface tension at the interface is

$$p_2 - p_1 = -\tau(\kappa_{\perp} + \kappa_{\parallel}) \quad (8)$$

A first approximation of κ_{\perp} is $2/b$; more accurate determination can be given, but it is not important to our analysis.

If we assume an interface at

$$x = Ut + \varepsilon e^{\sigma t} \cos ky \quad (9)$$

where $\varepsilon \ll 1$ and U is a constant velocity in the x direction we are led to the *ansatz* on the pressure,

$$p_1 = p_{10} - \frac{12\mu_1 U}{b^2}(x - Ut) + \varepsilon B_1(t)e^{kx} \cos ky \quad (10)$$

$$p_2 = p_{20} - \frac{12\mu_2 U}{b^2}(x - Ut) + \varepsilon B_2(t)e^{-kx} \cos ky \quad (11)$$

which satisfies Laplace's equation (4). Then, assuming no source term c , the velocity and pressure are related by

$$v = -\frac{b^2}{12\mu_1} \nabla p_1 = -\frac{b^2}{12\mu_2} \nabla p_2 \quad (12)$$

on the interface. To order ε , curvature κ_{\parallel} is given by

$$\kappa_{\parallel} = -\frac{\partial^2}{\partial y^2} x(t, y) = \varepsilon k^2 e^{\sigma t} \cos ky \quad (13)$$

and the x -component of velocity on the interface by

$$v = \frac{\partial x}{\partial t} = U + \varepsilon \sigma e^{\sigma t} \cos ky \quad (14)$$

If we assemble all these, we obtain the dispersion relation describing the growth of pattern of various wavenumbers (Saffman and Taylor, 1958),

$$\sigma = \frac{\tau b^2 k}{12(\mu_1 + \mu_2)} \left(\frac{12U(\mu_2 - \mu_1)}{\tau b^2} - k^2 \right) \quad (15)$$

Thus there is a dispersion relation $\sigma(k)$, with σ cubic in k , and pattern will grow for positive σ , that is if $U(\mu_2 - \mu_1) > 0$, then pattern will grow. This is the standard result: if one drives a less-viscous fluid into a more viscous fluid, fingers grow, but a viscous fluid driven into a less viscous fluid has a stable planar interface. There is a fastest growing wavenumber,

$$k^2 = \frac{4U(\mu_2 - \mu_1)}{\tau b^2} \quad (16)$$

In the degenerate case of the absence of surface tension, the interface is unstable to disturbances of all wavenumbers, and is most unstable to the largest wavenumbers, i.e. to disturbances at the finest scales. The resulting interface is fractal, and outside of our area of interest.

4.2 Model refinement: three fluids

It is clear from sections of embryonic lung tissue that there are two fairly distinct layers of mesenchyme in the lung. The inner mesenchyme, condensed

around the epithelium, has dense ECM and a high cell density. The outer layer is less structured, and we expect that it has different stress response (viscosity). A clear refinement of the model would be the inclusion of more than two different fluids. In Sect. 2, we made the simplifying assumption of two fluids (amniotic fluid and mesenchyme) with one interface between them. A more complicated model would incorporate the flow of *three* fluids, where fluid 1 represented the amniotic/luminal fluid, fluid 2 represented the dense mesenchyme that condenses around the epithelium, and fluid 3 represented the thinner outer mesenchyme. We suspect that such a model would more realistically mimic the lobar structure of the developing lung, if we make the correct assumptions about the relative viscosities of the three fluids. However, we have not found any experiments which enable us to make assumptions *a priori* on the relative viscosities (stress-growth response) of the inner and outer mesenchyme. One of the benefits of mathematical modeling is that it can lead to predictions of experimentally verifiable phenomena and quantities. We can use a little analysis of the model to make *predictions* of the relative viscosities of the inner and outer mesenchyme.

Suppose, therefore, that there are three fluids in the Hele-Shaw cell, with two well-defined nonintersecting simply-connected interfaces Γ_1 and Γ_2 . Again in the interests of simplicity, let us make the assumption of immiscibility of the inner and outer mesenchyme. Consider both interfaces to be moving at a constant velocity U in the x direction, as before, and let Γ_1 and Γ_2 be separated an average distance L . Then the interfaces influence each other through viscosity, though in the limit $L \rightarrow \infty$, they influence each other very little.

Assume, for this analysis, no complicating source term c , and let the interfaces be described by

$$\Gamma_1: x = Ut + \varepsilon e^{\sigma t} \cos ky \quad (17)$$

$$\Gamma_2: x = Ut + L + \varepsilon \alpha e^{\sigma t} \cos ky \quad (18)$$

where α is to be determined. Then Laplace's equation (4) must be satisfied in each fluid, and at each interface, there is a curvature condition

$$\Gamma_1: p_2 - p_1 = -\tau_1(\kappa_{\perp} + \kappa_{\parallel}) \quad (19)$$

$$\Gamma_2: p_3 - p_2 = -\tau_2(\kappa_{\perp} + \kappa_{\parallel}) \quad (20)$$

The *ansatz* for the pressure is then

$$p_1 = p_{10} - \frac{12\mu_1 U}{b^2} (x - Ut) + \varepsilon B_1(t) e^{kx} \cos ky \quad (21)$$

$$p_2 = p_{20} - \frac{12\mu_2 U}{b^2} \left(x - \frac{L}{2} - Ut \right) + \varepsilon (A_1(t) e^{kx} + A_2(t) e^{-kx}) \cos ky \quad (22)$$

$$p_3 = p_{30} - \frac{12\mu_3 U}{b^2} (x - L - Ut) + \varepsilon B_3(t) e^{-kx} \cos ky \quad (23)$$

which satisfies the Laplace equation (4). The velocities on the interfaces are now given by

$$\Gamma_1: v = -\frac{b^2}{12\mu_1} \nabla p_1 = -\frac{b^2}{12\mu_2} \nabla p_2 \quad (24)$$

$$\Gamma_2: v = -\frac{b^2}{12\mu_2} \nabla p_2 = -\frac{b^2}{12\mu_3} \nabla p_3 \quad (25)$$

and, to order ε ,

$$\Gamma_1: v = \frac{\partial x}{\partial t} = U + \varepsilon \sigma e^{\sigma t} \cos ky \quad (26)$$

$$\Gamma_2: v = \frac{\partial x}{\partial t} = U + \varepsilon \alpha \sigma e^{\sigma t} \cos ky \quad (27)$$

Putting these all together, determining the various coefficients A_1, A_2, B_1, B_3 , gives the two equations in α and σ ,

$$k^2 \tau_1 + \frac{12U}{b^2} (\mu_1 - \mu_2) + \frac{12\sigma}{b^2 k} \left(\mu_1 + \mu_2 \frac{\cosh kL - \alpha}{\sinh kL} \right) = 0 \quad (28)$$

$$k^2 \tau_2 + \frac{12U}{b^2} (\mu_2 - \mu_3) + \frac{12\sigma}{b^2 k} \left(\mu_3 + \mu_2 \frac{\cosh kL - \frac{1}{\alpha}}{\sinh kL} \right) = 0 \quad (29)$$

These are easily solved for $\sigma(k)$, the growth rate, and for α , the ratio of the amplitudes of the two interfaces. They are ill-behaved as $L \rightarrow 0$, due to the \sinh term. However, $\lim_{k \rightarrow 0} \sigma(k) = 0$. Equations (28) and (29) yield

$$A\sigma^2 + B\sigma + C = 0 \quad (30)$$

where

$$A = d_1 d_2 - c^2 \quad (31)$$

$$B = c_1 d_2 + c_2 d_1 \quad (32)$$

$$C = c_1 c_2 \quad (33)$$

and

$$c = \frac{\mu_2}{\sinh kL} \quad (34)$$

$$c_1 = \frac{b^2 k^3 \tau_1}{12} + Uk(\mu_1 - \mu_2) \quad (35)$$

$$c_2 = \frac{b^2 k^3 \tau_2}{12} + Uk(\mu_2 - \mu_3) \quad (36)$$

$$d_1 = \mu_1 + \mu_2 \coth kL \quad (37)$$

$$d_2 = \mu_3 + \mu_2 \coth kL \quad (38)$$

Note that

$$A = d_1 d_2 - c^2 = \mu_1 \mu_3 + \mu_2^2 + (\mu_1 + \mu_3) \mu_2 \coth kL > 0 \quad (39)$$

by suitable application of hyperbolic identities, and

$$B^2 - 4AC = c_1^2 d_2^2 + c_2^2 d_1^2 + 4c^2 > 0 \quad (40)$$

There are therefore, from (30, 40), two real solutions $\sigma_{1,2}(k)$. Zero is always a root of each, since $\lim_{k \rightarrow 0} \sigma(k) = 0$. We also know that σ depends on L , the distance between interfaces, only as $\mu_2 \coth kL$. Another observation we can make is that $\lim_{k \rightarrow \infty} \sigma(k) = -\infty$, so the interface is always stable to the shortest wavelength disturbances.

We can further determine the behavior of σ 's k -dependence. Let the two roots be designated σ_1 and σ_2 . Then

$$\frac{\partial \sigma_1}{\partial k}(0) = 0 \quad (41)$$

$$\frac{\partial \sigma_2}{\partial k}(0) = \frac{U(\mu_3 - \mu_1)}{\mu_3 + \mu_1} \quad (42)$$

$$\frac{\partial^2 \sigma_1}{\partial k^2}(0) = \frac{2UL(\mu_2^2 - \mu_2(\mu_1 + \mu_3) + \mu_1\mu_3)}{\mu_2(\mu_1 - \mu_3)} \quad (43)$$

$$\frac{\partial^2 \sigma_2}{\partial k^2}(0) = \frac{-8UL\mu_1\mu_3(\mu_2^2 - \mu_2(\mu_1 + \mu_3) + \mu_1\mu_3)}{\mu_2(\mu_1 - \mu_3)(\mu_1 + \mu_3)^2} \quad (44)$$

For a positive root of σ to exist, with multiplicity 1 or 2, we need $c_1 < 0$ or $c_2 < 0$, making $C < 0$ and/or $B < 0$. We can now make four observations on pattern:

- A necessary condition for pattern is that $\mu_1 < \mu_2$ or $\mu_2 < \mu_3$.
- A sufficient condition for pattern is that $\mu_3 > \mu_1$, independent of μ_2 .
- It is not a necessary condition for pattern that $\mu_3 > \mu_1$, though it is sufficient.
- If $\mu_3 < \mu_1$, a sufficient condition for pattern is that

$$\mu_2^2 - \mu_2(\mu_1 + \mu_3) + \mu_1\mu_3 > 0 \quad (45)$$

This is satisfied as long as the viscosities are not monotonically decreasing.¹

These observations indicate that only when viscosities are monotonically decreasing in the direction of fluid flow does pattern *not* form. It is *not* the case that a monotonic increase in viscosity is necessary for pattern to grow; all that is required is that across one of the interfaces, viscosity increases in the direction of flow.

Typical dispersion relations are shown in Fig. 3, which shows $\sigma(k)$ for all 6 possible rankings of the magnitudes of three different viscosities, with positive velocity U , i.e. fluid being driven from region 1 into 2 and 2 into 3. Again, pattern forms for some band of wavenumbers in all cases except where

¹ Proof: Let $\mu_2 = \mu_3 + \delta_1$ and $\mu_1 = \mu_2 + \delta_2$. Then $\mu_2^2 - \mu_2(\mu_1 + \mu_3) + \mu_1\mu_3 = -\delta_1\delta_2$.

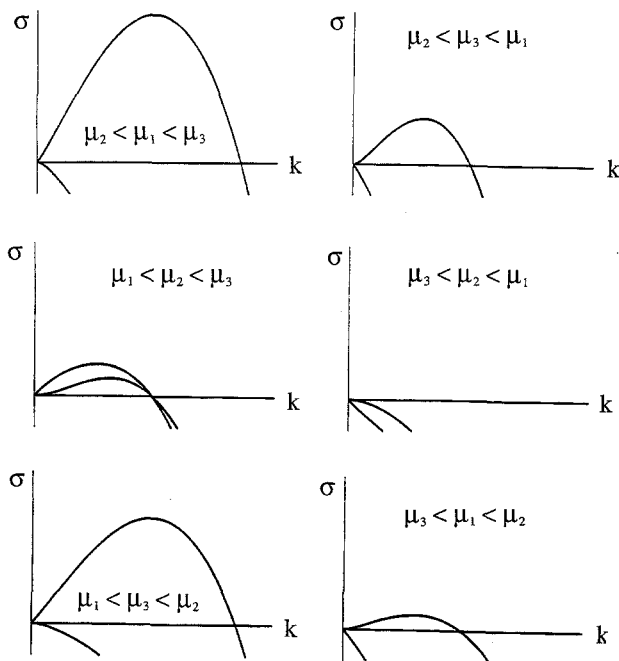


Fig. 3. Typical dispersion relation $\sigma(k)$ with two interfaces. Representative curves are given for all possible orderings of the magnitudes of three viscosities. In all such cases pattern forms, except in the case where $\mu_1 > \mu_2 > \mu_3$, i.e. monotonically decreasing viscosity

fluid viscosity is monotonically decreasing outwards. Pattern grows wherever $\sigma(k) > 0$, and the amplitude relation between disturbances on the two interfaces is given by $\alpha(k)$, shown in Fig. 4 for the two viscosity configurations most relevant to the problem of modeling the lung, i.e. those where μ_1 is negligible.

In the absence of data distinguishing the stress-growth responses of the inner and outer mesenchyme, we cannot make many quantitative predictions based on the assumed different properties of these two tissues. We can, however, make qualitative predictions: we observe that the amplitude ratio α can be *negative* in the case where $\mu_1 < \mu_2 < \mu_3$, meaning disturbances can grow where the inner interface and the outer interface are *out of phase*. Considering that this would, if pursued by the organism, lead to lumps of mesenchyme, rather than to a mesenchyme which evenly enfolds the lung, it is unlikely, based on this simple analysis of the model, that the viscosity of the outer mesenchyme is greater than that of the inner mesenchyme. Furthermore, the case $\mu_1 < \mu_3 < \mu_2$, which has only one positive root σ , has for that root an amplitude ratio $\alpha < 1$ for $k > 0$, which means pattern on the outer interface is of smaller amplitude than on the inner interface, as seen *in vivo/vitro*. We conclude that it is probable that the outer mesenchyme has a greater proliferative response to stress (lower tissue viscosity) than the inner mesenchyme.

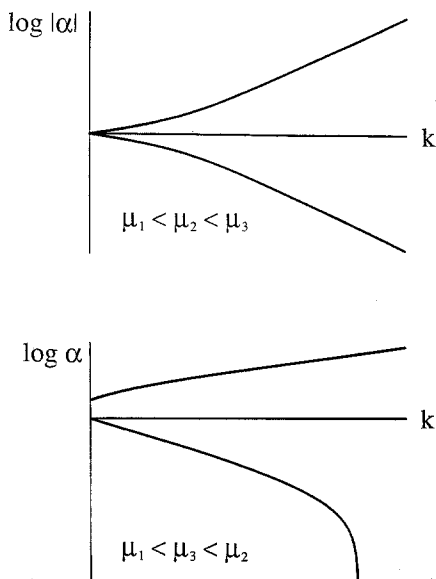


Fig. 4. Amplitude-wavenumber relation $\alpha(k)$ for two interfaces, for the specific case where $\mu_1 < \mu_3$ and $\mu_1 < \mu_2$, the cases which are relevant to lung growth. In the case where $\mu_1 < \mu_2 < \mu_3$, one of the roots of α is negative, indicating that pattern can grow on the two interfaces such that they are out of phase with each other, whereas in the case of the other root of α , and always in the case where $\mu_1 < \mu_3 < \mu_2$, the growing patterns on the two interfaces are in phase with each other

5 Numerical analysis

It is claimed (Bensimon et al. 1986) that diffusion-limited aggregation (DLA) with surface tension is a correct mathematical analogy of viscous fingering. Along these lines, Kadanoff (1985) and Liang (1986) developed a Monte Carlo "pedestrian" algorithm for simulating viscous fluid flow. Fluid flux is computed by probability densities, which are computed by averaged random walks. The random walks originate from loci on the boundary or the interface of equal probability, and terminate on the interface. Each random walk carries with it a flux which depends on its origin (boundary or interface itself) and on the local curvature of the interface. For higher values of the control parameter B (6, 16), which is proportional to surface tension, the interface-interface walks are responsible for a greater proportion of the motion of the boundary. For details of the method and its accuracy, see (Kadanoff 1985; Liang 1986).

The advantage of the Monte Carlo method over the more customary boundary integral method is that for small values of the control parameter B , near the DLA limit, the flow is approaching indeterminacy, and is highly sensitive to noise of a wide range of frequencies. At greater values of B , noise is less important, and the flow more deterministic. This, however, is adequately handled by the Monte Carlo method simply by increasing the number of visits

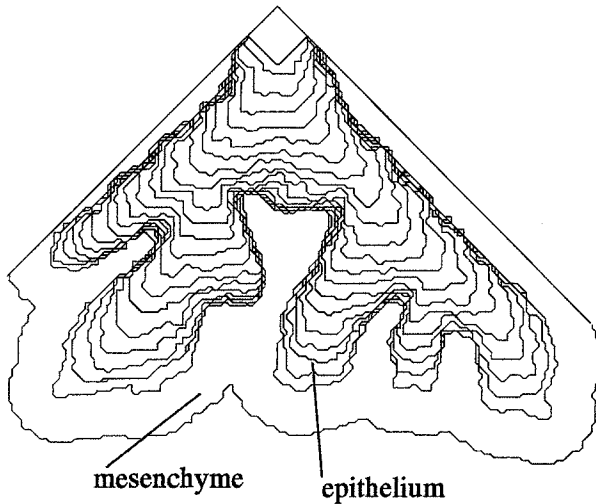


Fig. 5. Representative simulation of viscous fingering model of initial lung development. Contours represent the shape of the interface over time, starting with the smallest curve (an arbitrary initial condition). The lung is considered to be rigidly bounded on two sides, and free to expand on the third. Control parameter $B = 0.02$

by a random walk required for a given spot on the interface to move. The method can be trivially generalized to three dimensions, though cost prevents its use in three dimensions in this study.

In the interest of studying the simplest possible cases, we assumed for the simulations that the intrinsic growth rate c in equations (2, 4, 5, 7) was zero, that is, that the entire driving force was externally imposed, and simplified the outer interface to maintain a constant distance from the inner interface. A representative simulation is shown in Fig. 5. In this simulation, the lung is considered to be rigidly confined on two sides, and free to expand in the general caudal direction.

The overall pattern is primarily dependent on the boundary conditions and the dimensionless parameter B , and we have extensively explored the effect of both. Given the same boundary conditions as in Fig. 5, a very similar pattern evolved from a variety of initial conditions, and for a range of B from approximately 0.01 to 0.05. For B outside of that order of magnitude, the pattern was substantially different, either with branching of nonuniform size, or not enough branching. Variation was observed in the patterns, but the overall size, size range, time course, and number of branchings in our simulations depended only on the control parameter. The actual boundary conditions in the human lung in its embryonic period are, of course, in three dimensions, and in order to accurately duplicate them, one would have to account for the other organs nearby, such as the heart, liver, and esophagus (two of which, being asymmetrically placed, must surely affect the symmetry of the second branching). In addition, the entire organism is growing as the lung

is developing, and this provides, in effect, a moving boundary condition, which could be complicated to describe accurately in space and time.

6 Discussion

Our simulations show that a very simple fluid model captures many of the essential features of the early embryonic morphogenesis of the lung. Our model exhibits tip splitting, as does the embryonic lung, and is capable of reproducing the 2–3 split at the second branching of the bronchial tree, even without the inclusion of known *in vivo* boundary conditions (such as the presence of the esophagus and heart). Although the qualitatively and quantitatively observed behavior has been achieved with a two-dimensional simulation, we believe similar behavior will be found in a similar but much more mathematically complex and numerically costly three-dimensional model. Furthermore, our simulations demonstrated that even without the biologically realistic source term $\nabla \cdot u = c > 0$, representing an intrinsic growth rate without stress, the fluid model formulation provides reasonable qualitative and quantitative predictions of the tissue deformations and pattern formation.

The model presented in this paper predicts the early embryonic branching of the presumptive lung, but in its present form, it cannot account for the later stages of development, which are characterized by many more different types of tissues, depending on the developmental age of the relevant portion of lung, as well as very different physical properties. For example, as the lung develops, the bronchi enlarge and develop cartilage. The cartilage must make the bronchi substantially stiffer, and it is unlikely that a purely fluid model can account for the expansion of the airways during the later development. The later development, in which the airways enlarge proportional to the volume flux of air that they will carry, must also involve stress-stimulated growth, the stress coming from the fetal breathing movements which are essential to healthy pulmonary development.

The latest stage of lung development, the formation of the acini, will certainly be governed by a different mechanism, since the acini are structurally and geometrically very different from the bronchial tree. Furthermore, the acini develop both prenatally and postnatally: they develop both in a fluid-filled pressurized state and an air-filled state, which are mechanically very different.

Perhaps the main point of our theory of lung development is that it makes predictions which can be experimentally tested. We have used our model to predict that the viscosity (stress-growth response) of the inner, denser mesenchyme is greater than that of the outer mesenchyme. Another prediction comes from the fact that low Reynolds number flow is highly sensitive to boundary conditions. There have already been studies of embryonic lung tissues *in vitro*, and these could be adapted to include boundary conditions that would be more tractable. Since viscous fingering in a Hele-Shaw cell with

rigid sidewalls a set distance apart is known to have a single stable finger for moderate values of the control parameter B , cultured lung epithelium and fibroblasts should organize into a single finger, if confined to a channel in their medium of appropriate width. Another possible experiment would be to alter the pressure difference between the two tissues artificially, as in the *in vivo* experiments on the later stages of development (Alcorn et al. 1977; Fewell et al. 1983; Moessinger et al. 1990). A higher pressure difference should lead to finer and more irregular branching of the embryonic bronchial tree, and a lower pressure difference to coarser and less frequent branching.

This methodology of addressing the stress responses of developing tissues should be applicable to a number of similar systems, such as the branching development of salivary glands. Numerous other tissues throughout the body have been found to be more or less strongly dependent on mechanical stress effects (Curtis and Seehar, 1978; Folkman and Moscona, 1978), and we expect that such stress responses may be a general feature of branching morphogenesis, though we have not yet found experimental evidence of a specific stress-growth response in any specific glandlike tissue but the lung.

What our model does not address is the specific chemical mechanisms and the other details of cellular responses to stresses and to each other, issues which have been studied in detail elsewhere. Our model is concerned with tissue deformations at the level of stress and growth, rather than at the level of, for example, GAG synthesis and degradation, in the same way that an ethologist may study insect movements in terms of velocities, without addressing which pheromones are directing the movements. Our mechanical approach offers a different and new perspective on lung development, and on branching organogenesis in general.

Appendix: parameter estimation

In this paper, we have introduced a new concept, that of the viscosity of developing tissues, defined, as is fluid viscosity, as the ratio between stress and strain (growth) rate. We can estimate the magnitude of fetal lung viscosity from the experiments of Liu et al. (1992) and Bishop et al. (1993) who give data relating the strain they imposed on the tissues and the resulting increase in growth rate over control. Under the assumptions that cyclically deformed tissues average their stress response over time and that their fast elastic response is linear, and supposing their modulus of elasticity to be of the order of 10^7 dyn/cm² (close to that of other soft tissues), we obtain the same estimate for viscosity from the data of both studies: $\mu \sim 10^{10}$ to 10^{11} dyn-sec/cm².

The flow of tissues in the developing lung is extremely slow, and on a very small length scale. We can estimate the Reynolds number of the flow,

$$Re = \frac{\rho LU}{\mu} \quad (46)$$

from the known time and length scales, the density of water, and the above viscosity, to be about $\text{Re} \sim 10^{-21}$, which is extremely low and trivially justifies a Stokes' approximation.

The most unstable wavenumber of growing pattern on the interface between the two fluids is given by (16). Assuming that the domain is perhaps one order of magnitude wider than the plate separation, and estimating these length scales, the viscosity, velocity, and surface tension (estimate $\tau \sim 10^4 \text{ gm/cm}^2$, of the same order of magnitude as cornea), suggests that the appropriate range of the control parameter $B = \pi^2 b^2 \tau / (3a^2 \mu U)$ is approximately 0.01 to 0.1. We found that the most lung-like patterns formed in our simulations when B was between 0.01 and 0.05.

Acknowledgements. This work was supported in part by grant DMS-9306108 from the National Science Foundation (S.R.L.) and by grant 2 P41 RR01243-12 from the National Institutes of Health (J.D.M.). We are grateful for critical input from Tom Daniel and Garry Odell.

References

1. D. T. Alcorn, M. Adamson, T. F. Lambert, J. E. Mahoney, B. C. Ritchie, and P. M. Robinson. Morphological effects of chronic tracheal ligation and drainage in the fetal lamb. *J. Anat.*, 123: 649–660, 1977.
2. T. Alescio and A. Cassini. Induction in vitro of tracheal buds by pulmonary mesenchyme grafted on tracheal epithelium. *J. Exp. Zool.*, 150: 83–94, 1962.
3. D. Bensimon, L. Kadanoff, S. Liang, B. Shraiman, and C. Tang. Viscous flows in two dimensions. *Reviews of Modern Physics*, pages 977–999, 1986.
4. J. E. Bishop, J. J. Mitchell, P. M. Absher, L. Baldor, H. A. Geller, J. Woodcock-Mitchell, M. J. Hamblin, P. Vacek, and R. B. Low. Cyclic mechanical deformation stimulates human lung fibroblast proliferation and autocrine growth factor activity. *Am. J. Respir. Cell Mol. Biol.*, 9(2): 126–133, August 1993.
5. R. G. Crystal, J. B. West, P. J. Barnes, N. S. Cherniack, and E. R. Weibel. *The Lung: Scientific Foundations*. Raven Press, New York, 1991.
6. A. S. G. Curtis and G. M. Seehar. The control of cell division by tension or diffusion. *Nature*, 274: 52–53, 1978.
7. J. E. Fewell, A. Hislop, J. A. Kitterman, and P. Johnson. Effect of tracheostomy on lung development in fetal lambs. *J. Appl. Physiol.*, 55: 1103–1108, 1983.
8. J. E. Fewell and P. Johnson. Upper airway dynamics during breathing and during apnoea in fetal lambs. *J. Physiol. Lond.*, 339: 495–504, June 1983.
9. J. Folkman and A. Moscona. Role of cell shape in growth control. *Nature*, 273: 345–349, 1978.
10. W. A. Hodson. *Development of the Lung*, volume 6 of *Lung Biology in Health and Disease*. Marcel Dekker, 1977.
11. A. M. Jetten. Growth and differentiation factors in tracheobronchial epithelium. *Am. J. Physiol.*, 260(6 part 1): L361–L373, 1991.
12. L. Kadanoff. Simulating hydrodynamics: a pedestrian model. *Journal of Statistical Physics*, 39(3/4): 267–283, 1985.
13. D. A. Kessler, J. Koplik, and H. Levine. Pattern selection in fingered growth phenomena. *Advances in Physics*, 37(3): 255–339, 1988.
14. J. Kolega. The movement of cell clusters in vitro: Morphology and directionality. *J. Cell Sci.*, 49: 15–32, 1981.
15. L. D. Landau and E. M. Lifshitz. *Fluid Mechanics*. Pergamon Press, 1959.

16. S. Liang. Random-walk simulations of flow in Hele Shaw cells. *Physical Review A*, 33(4): 2663–2674, April 1986.
17. M. Liu, S. J. M. Skinner, J. Xu, R. N. N. Han, A. K. Tanswell, and M. Post. Stimulation of fetal rat lung cell proliferation in vitro by mechanical stretch. *Am. J. Physiol.*, 263: L363–L383, 1992.
18. S. E. McGowan. Extracellular matrix and the regulation of lung development and repair. *FASEB J.*, 6(11): 2895–2904, 1992.
19. A. C. Moessinger, R. Harding, T. M. Adamson, M. Singh, and G. Kim. Role of lung liquid volume in growth and maturation of the fetal sheep lung. *J. Clin. Invest.*, 86: 1270–1277, 1990.
20. J. D. Murray. *Mathematical Biology*. Springer-Verlag, 1989. 2nd corrected edition 1993.
21. G. H. Nelson. *Pulmonary Development: Transition from Intrauterine to Extrauterine Life*, volume 27 of *Lung Biology in Health and Disease*. Marcel Dekker, 1985.
22. G. F. Oster, N. Shubin, J. D. Murray, and P. Alberch. Evolution and morphogenetic rules: The shape of the vertebrate limb in ontogeny and phylogeny. *Evolution*, 42: 862–884, 1988.
23. P. G. Saffman and G. I. Taylor. The penetration of a fluid into a porous medium or Hele-Shaw cell containing a more viscous liquid. *Proceedings of the Royal Society of London, Series A, Mathematical and Physical Sciences*, 245: 312–329, 1958.
24. S. Takeuchi. Wound healing in the cornea of the chick embryo. IV. Promotion of the migratory activity of isolated corneal epithelium in culture by the application of tension. *Dev. Biol.*, 70: 232–240, 1979.
25. G. Vilos and G. C. Liggins. Intrathoracic pressures in fetal sheep. *Journal of Developmental Physiology*, 4: 247–256, 1982.
26. E. R. Weibel. Fractal geometry: a design principle for living organisms. *Am. J. Physiol.*, 261: 361–369, 1991.